Chapter 4: Instantaneous Kinematic Analysis

The instantaneous kinematic analysis of a manipulator defines the direction and magnitude (translational and rotational) of impending motion at a specific point in time. This analysis is position dependent, and assumes apriori knowledge of the position information. From the position kinematic analysis, a kinematic transformation between joint space and tool space can be represented as:

$$\mathbf{x} = f(\theta) \tag{4.1}$$

Instantaneous or velocity analysis follows directly from the position analysis. Here, the input velocity vector, ω is mapped into the output space velocity vector, **v**, by the matrix, **J** called the Jacobian of the manipulator:

$$\mathbf{v} = \mathbf{J}\omega . \tag{4.2}$$

This matrix equation demonstrates that the Jacobian is necessarily a linear relationship between the input and output velocities. Obtaining the Jacobian, however, may involve a complex process. When the vector function *f* from the position analysis is available explicitly, velocity analysis (the Jacobian) results from direct differentiation. However, in most parallel manipulators the kinematic equations are implicit, making differentiation non-trivial. A number of alternative methods are available for Jacobian determination. For example, the Jacobian can be created from a set of linear velocity equations based on the known manipulator position information. Screw theory provides another well-known approach to developing a system Jacobian. However, these approaches result in several complications when applied to parallel manipulators. In this analysis, although the kinematic position equations are implicit, direct differentiation is used to obtain the Jacobian matrix.

The system Jacobian plays a central role in the kinematics of a robotic manipulator. As shown in Eq. 4.2 above, it is used to define the relationship between the actuated input velocities and the output or tool velocities. It is even more important in quantifying the performance of a manipulator. Two key performance measures, the size and continuity of the available (singularity-free) workspace and the manipulability or dexterity measure throughout the workspace, are contained in the algebra of the Jacobian matrix.

Once the Carpal Wrist's Jacobian is derived, the performance measures of the new device can be evaluated. Results from these evaluations will play an important role in comparing the new robotic wrist to current wrist technology.

4.1 Discussion of Singularities

One of the primary interests in manipulator velocity analysis is to determine the presence and location of any singular positions. The physical implication of a singular position is that the manipulator loses one or more degrees of freedom of output motion. The mathematical cause is a loss in the number of linearly independent columns of the Jacobian matrix. For a square Jacobian, the result is that the inverse no longer exists and the determinate goes to zero. For a non-square Jacobian, full rank is lost. As described in the introduction to robotic manipulators, it

is often convenient to consider the motion of a manipulator system in two parts; a regional pointing system, or robot arm, and an orienting system, or robot wrist. Singularities can exist in either of these two systems, or they may arise in the interface of the two systems (Williams, 1994). Wrist partitioning allows the singularity effects of the Carpal Wrist to be examined independent of any specific robot arm or positioning system. The partitioning method requires the wrist to be spherical, with all the wrist axes intersecting at a common point (Wampler, 1988). This partitioning system applies to the Carpal wrist, since it can be operated in a spherical nature, i.e., output (tool) orientations take place about a fixed or common center (Salerno et. al., 1995).

Singularities can be classified into two categories based on where they occur in the manipulator workspace; boundary and interior singularities. Boundary singularities occur at the boundary of the manipulator's workspace, i.e., when the manipulator is fully extended. Interior singularities occur within the workspace boundaries of the manipulator, and are frequently caused by the manipulator joint axes becoming parallel in a typical manipulator. Singularities that exist at the workspace boundaries are usually of less consequence, since they occur when the manipulator is at its maximum reach. These singularities must simply be accepted as a practical limitation of all devices. However, interior singularities create the greatest concern since they will interrupt normal operation of the manipulator. A wrist free of interior singularities will be referred to as a singularity-free wrist.

4.1.1 Singularities in Current Robotic Wrists

Interior wrist singularities can severely handicap manipulator performance. For example, these may create a number of unreachable positions, resulting in difficult path planning and perhaps controller errors. Avoiding singular regions, when it can be done successfully, can be expensive in terms of robot operation. In an effort to avoid singularity zones, the workspace of the manipulator is often reduced. For these reasons, singularity avoidance and singularity-free robotic wrists have been proposed by many researchers, including Stanisic and Duta (1990), Wampler (1989), Rosheim (1990), Milenkovic (1987), Remis and Stanisic (1993), and others. The common approach to eliminating wrist singularities involves introducing one or more redundant degrees of freedom. For example, Stanisic and Duta propose a symmetrically actuated, double pointing wrist system (1990). This wrist provides tool pointing, a two degree-of-freedom specification, with three intersecting revolute axes. The wrist proposed by Rosheim (1990) and Milenkovic (1987) consists of a Double Cardan joint structure, or a four degree-of-freedom device providing tool pointing, a two degree-of-freedom task.

Most of the research in singularity-free wrist design has involved serial devices. While parallel devices have many advantages in robotic applications, such as a high strength and low weight, they are generally thought to be limited in workspace and range of motion. However, when considering the singularity-free workspace, the Carpal Wrist, a parallel device, will be shown to be superior to many serial wrists.

4.2 Discussion of Dexterity

Even if a manipulator is not singular at a point, it may be nearly singular. Mathematically, this is demonstrated in the Jacobian matrix becoming poorly or ill-conditioned. Physically, one or more degrees of freedom may be severely compromised. The ability to move well in all directions is traditionally measured as good dexterity. Dexterity in robotic manipulators has been studied by many researchers, with many definitions proposed. One of the first methods of quantifying dexterity was the number of redundant degrees of freedom. Since a singularity occurs when the number of linearly independent columns falls below the number of rows, an increase in redundancy (i.e., an increase in the number of columns), increases the opportunity for independent columns. Another dexterity definition commonly applied is the Jacobian determinant, which measures the magnitude of the Jacobian at a particular position. Since the Jacobian matrix defines the relative stretching between the input to output velocities, the magnitude of the Jacobian, found as its determinant, gives an indication of overall dexterity. Examples of research that has used the determinant as an indication of dexterity include Paul and Stevenson, (1983), and Stanisic and Duta, (1990). As the magnitude of the Jacobian determinant approaches zero, the implication that there is at least one output direction that becomes unreachable. This dexterity measure is often used to define a dexterous workspace of a manipulator as the workspace where the Jacobian determinant is greater than some limiting value. One drawback to this definition is the lack of information about control authority among the independent output motions. For example, when dexterity in one of the manipulator dof's approaches zero while another approaches infinity, the overall determinant may not indicate the loss of motion. Therefore, a third dexterity definition has been proposed as the ratio of maximum to minimum singular values, resulting from a singular value decomposition of the Jacobian matrix. For this measure, a ratio near one is assumed to be dexterous, while a singular position is indicated by the ratio going to infinity. This measure also contains drawbacks, for example when all directions approach singular positions uniformly, the ratio will remain constant.

A combination of the determinant-based dexterity and the singular-value-decomposition-based dexterity can be applied to avoid errors occurring in each individually (Soper et al., 1997). This is demonstrated in Table 4.1:

Table 4.1: Combining Two Dexterity Measures

		$\lvert\det J\rvert$	
		$\ll 1$	finite
$\sigma_{max} / \sigma_{min}$	$\gg 1$	low dexterity	low dexterity
	≈ 1	low dexterity	high dexterity

Note that high manipulator dexterity is implied when the determinant measure is finite and the singular value ratio measure is approximately one.

A descriptive dexterity definition that avoids many of the defects of previous definitions is presented by Soper et al., (1997). The essence of this dexterity definition is that the dexterity, *D*, gives the relative stretching between the input and output velocity vectors.

$$D = \frac{\|\mathbf{v}\|}{\|\omega\|} = \frac{1}{\mu} \tag{4.3}$$

where *D* is the definition of dexterity applied in this paper and μ is the mechanical advantage. Expanding this definition for three potential manipulator kinematics gives explicit equations for *D*:

For a square nonsingular Jacobian,

$$D = \sqrt{\mathbf{v}^T\mathbf{v}\left(\mathbf{v}^T\left(\mathbf{J}^{-1}\right)^T\mathbf{J}^{-1}\mathbf{v}\right)^{-1}} \tag{4.4}$$

For a tall nonsingular Jacobian,

$$D = \sqrt{\mathbf{v}^T\mathbf{v}\left(\mathbf{v}^T\mathbf{J}\left[\left(\mathbf{J}^T\mathbf{J}\right)^{-1}\right]^T\left(\mathbf{J}^T\mathbf{J}\right)^{-1}\mathbf{J}^T\mathbf{v}\right)^{-1}} \tag{4.5}$$

For a short nonsingular Jacobian,

$$D = \sqrt{\mathbf{v}^T\mathbf{v}\left(\mathbf{v}^T\left(\mathbf{R}^{-1}\right)^T\mathbf{R}^{-1}\mathbf{v}\right)^{-1}} \tag{4.6}$$

where *R* is stretch matrix resulting from the matrix polar decomposition,

$$\mathbf{RQ}\omega = \mathbf{v} \tag{4.7}$$

A given robotic architecture is deemed “dexterous” if the manipulator is able to adequately and effectively position and orient a tool within its reachable workspace. Since the ability to pose (position and orient) is the robot’s fundamental task, the parameter for evaluating this, referred to as the “dexterous measure,” is an extremely important parameter for use in selecting and evaluating manipulators. The dexterous measure differs from the property dexterity in that dexterity is a function of manipulator position and velocity direction, while the dexterous measure provides a single quantitative value of the robot’s overall ability to move. Canfield et al., (1997) demonstrate that uniformity of dexterity is the essential feature of a dexterous manipulator and define the dexterous measure as the standard deviation of a chosen dexterity parameter evaluated over the workspace.

Using these definitions, the dexterity of the Carpal Wrist is mapped over the workspace for several general tasks. The overall dexterity, or dexterous measure will also be evaluated and a comparison in dexterous performance between the Carpal Wrist and traditional robotic wrists will be presented.

4.3 Closed-Form Jacobian

The Jacobian of the Carpal Wrist architecture is generated through differentiation of the position equations. Figure 4.1 shows the diagram of the kinematic model of the Wrist. The

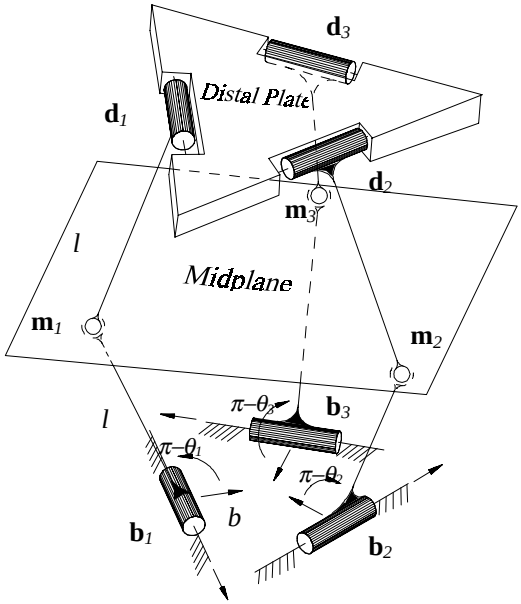

Figure 4.1: Kinematic Diagram of the Carpal Wrist

inputs to this model are the angles, θ_1, θ_2, and θ_3, of the three legs defined by vectors leading from nodes $\mathbf{b}_i$ to $\mathbf{m}_i$, $i = 1\ldots3$ and measured from the basal plane. The three mid-nodes, $\mathbf{m}_1$, $\mathbf{m}_2$, and $\mathbf{m}_3$ define a plane of symmetry between the basal and distal plates of the wrist. The outputs of this three degree-of-freedom wrist are control of the orientation of the distal plate normal (two dof) and the plunge distance from the midplane to the distal plate, measured along the distal plate normal (one dof). Due to the symmetry of the wrist, orientation and plunge of the output or distal plane can be defined from the orientation and plunge of the midplane. Therefore, closed-form equations defining the midplane with respect to the base plane are sufficient to solve for the Wrist Jacobian. Note that this is an intermediate solution to the forward position kinematic solution developed in Chap. 3. The change in deriving position equations which locate the symmetric midplane, (and thus contain the information required to locate the distal plate), is employed to make differentiation of the position equations tractable.

First, the equations for the midplane normal and the plunge distance are determined.

$$\mathbf{N} = \begin{Bmatrix} N_x \\ N_y \\ N_z \end{Bmatrix} = \begin{Bmatrix} \frac{\sqrt{3}l^2}{2}\left(s_1\left(\frac{-2b}{l} - c_2 - c_3\right) + s_2\left(\frac{b}{l} + c_3\right) + s_3\left(\frac{b}{l} + c_2\right)\right) \\ \frac{l^2}{2}\left(s_1\left(-c_2 + c_3\right) + s_2\left(\frac{-3b}{l} - 2c_1 - c_3\right) + s_3\left(\frac{3b}{l} + 2c_1 + c_2\right)\right) \\ \frac{\sqrt{3}l^2}{2}\left(\frac{3b^2}{l^2} + \frac{2b}{l}\left(c_1 + c_2 + c_3\right) + \left(c_1c_2 + c_1c_3 + c_2c_3\right)\right) \end{Bmatrix} \tag{4.8}$$

$$p_d = \left[\left(\frac{\left(b + lc_1\right)\left(s_1\left(\frac{2b}{l} - c_2 - c_3\right) + s_2\left(\frac{b}{l} + c_3\right) + s_3\left(\frac{b}{l} + c_2\right)\right)}{6b^2 + c_1\left(\frac{2b}{l} + 2c_2 + 2c_3\right) + c_2\left(\frac{4b}{l} + 2c_3\right) + \frac{4b}{l}c_3}\right) + \left(ls_1\right)\right] \tag{4.9}$$

where $\mathbf{N}$ is the midplane normal, p_d is the plunge distance, b and l are the length parameters shown in Fig. 4.1, and c_i and s_i are $\cos(\theta_i)$ and $\sin(\theta_i)$, for $i = 1,\ldots,3$. The midplane normal defines the two degree-of-freedom pointing control the Wrist provides and, therefore, only contains two independent output parameters which will be defined in the unit normal of the

midplane. The three degree-of-freedom output of the Wrist can be completely described then with the two dimensional midplane unit normal and the scalar plunge distance.

$$\hat{\mathbf{N}} = \frac{\mathbf{N}}{|\mathbf{N}|} = \begin{Bmatrix} N_x \Big/ \sqrt{N_x^2+N_y^2+N_z^2} \\ N_y \Big/ \sqrt{N_x^2+N_y^2+N_z^2} \\ N_z \Big/ \sqrt{N_x^2+N_y^2+N_z^2} \end{Bmatrix} = \begin{Bmatrix} \hat{N}_x \\ \hat{N}_y \\ \hat{N}_z \end{Bmatrix}. \tag{4.10}$$

Now, the output of the three degree-of-freedom wrist may be expressed as functions of the input angles through the first two components of the midplane unit normal and the plunge distance:

$$\begin{aligned} \hat{N}_x &= f_1(\theta_1,\theta_2,\theta_3) \\ \hat{N}_y &= f_2(\theta_1,\theta_2,\theta_3) \\ p_d &= f_3(\theta_1,\theta_2,\theta_3) \end{aligned}. \tag{4.11}$$

The Jacobian can be populated by taking derivatives of these three outputs, which are expressed as functions of the input angles,

$$\mathbf{J} = \begin{bmatrix} \partial\hat{N}_x/\partial\theta_1 & \partial\hat{N}_x/\partial\theta_2 & \partial\hat{N}_x/\partial\theta_3 \\ \partial\hat{N}_y/\partial\theta_1 & \partial\hat{N}_y/\partial\theta_2 & \partial\hat{N}_y/\partial\theta_3 \\ \partial p_d/\partial\theta_1 & \partial p_d/\partial\theta_2 & \partial p_d/\partial\theta_3 \end{bmatrix} \tag{4.12}$$

with

$$\partial\hat{N}_x/\partial\theta_i = \frac{\left(\partial N_x/\partial\theta_i \left(N_y^2+N_z^2\right) - \partial N_y/\partial\theta_i\, N_x N_y - \partial N_z/\partial\theta_i\, N_x N_z\right)}{\left(N_x^2+N_y^2+N_z^2\right)^{3/2}} \tag{4.13}$$

$$\partial\hat{N}_y/\partial\theta_i = \frac{\left(\partial N_y/\partial\theta_i \left(N_x^2+N_z^2\right) - \partial N_x/\partial\theta_i\, N_x N_y - \partial N_z/\partial\theta_i\, N_y N_z\right)}{\left(N_x^2+N_y^2+N_z^2\right)^{3/2}} \tag{4.14}$$

$$\partial p_d/\partial\theta_i = \frac{\left(-N_x m_{ix}\, \partial N_z/\partial\theta_i + N_x N_z\, \partial m_{ix}/\partial\theta_i + N_z m_{ix}\, \partial N_x/\partial\theta_i + N_z^2\, \partial m_{ix}/\partial\theta_i\right)}{N_z^2} \tag{4.15}$$

and

$$\begin{aligned} \partial N_x/\partial\theta_1 &= \sqrt{3}l^2/2\, c_1\left(-2b/l - c_2 - c_3\right) \\ \partial N_x/\partial\theta_2 &= \sqrt{3}l^2/2\left(s_1 s_2 - s_2 s_3 + c_2\left(b/l + c_3\right)\right) \\ \partial N_x/\partial\theta_3 &= \sqrt{3}l^2/2\left(s_1 s_3 - s_2 s_3 + c_3\left(b/l + c_2\right)\right) \end{aligned} \tag{4.16}$$

$$\begin{aligned} \partial N_y/\partial\theta_1 &= l^2/2\left(-c_1 c_2 + c_1 c_3 + 2 s_1 s_2 - 2 s_3 s_1\right) \\ \partial N_y/\partial\theta_2 &= l^2/2\left(s_1 s_2 - s_2 s_3 - 2 c_1 c_2 - c_2 c_3 - 3b/l\, c_2\right) \\ \partial N_y/\partial\theta_3 &= l^2/2\left(-s_1 s_3 + s_2 s_3 + 3b/l\, c_3 + 2 c_1 c_3 + c_2 c_3\right) \end{aligned} \tag{4.17}$$

$$\begin{aligned} \partial N_z/\partial\theta_1 &= -\sqrt{3}l^2/2\, s_1\left(2b/l + c_2 + c_3\right) \\ \partial N_z/\partial\theta_2 &= -\sqrt{3}l^2/2\, s_2\left(2b/l + c_1 + c_3\right) \\ \partial N_z/\partial\theta_3 &= -\sqrt{3}l^2/2\, s_3\left(2b/l + c_1 + c_2\right) \end{aligned} \tag{4.18}$$

$$\begin{aligned} \partial m_{ix}/\partial\theta_1 &= -ls_1; \partial m_{iy}/\partial\theta_1 = 0; \partial m_{iz}/\partial\theta_1 = lc_1 \\ \partial m_{ix}/\partial\theta_2 &= 0; \partial m_{iy}/\partial\theta_2 = 0; \partial m_{iz}/\partial\theta_2 = 0 \\ \partial m_{ix}/\partial\theta_3 &= 0; \partial m_{iy}/\partial\theta_3 = 0; \partial m_{iz}/\partial\theta_3 = 0 \end{aligned} \quad . \tag{4.19}$$

These equations represent a closed-form expression for the Jacobian as a function of the three input angles. This Jacobian gives the output velocity of the wrist as:

$$\begin{Bmatrix} \dot{\hat{N}}_x \\ \dot{\hat{N}}_y \\ \dot{p}_d \end{Bmatrix} = \mathbf{J} \begin{Bmatrix} \dot{\theta}_1 \\ \dot{\theta}_2 \\ \dot{\theta}_3 \end{Bmatrix}. \tag{4.20}$$

The *x* and *y* components of the midplane unit normal can be alternatively described by the two angles, α and $\beta/2$, as demonstrated in Fig. 4.2 and the following equations:

$$\begin{aligned} \hat{N}_x &= s(\beta/2)c\alpha \\ \hat{N}_y &= s(\beta/2)s\alpha \end{aligned} \tag{4.21}$$

Solving for these angles results in:

$$\begin{aligned} \alpha &= \arg\left(\hat{N}_x + i\hat{N}_y\right) \\ \left(\beta/2\right) &= \sin^{-1}\sqrt{\hat{N}_x^2 + \hat{N}_y^2} \end{aligned} . \tag{4.22}$$

Here, α and $\beta/2$ define the midplane normal. Due to symmetry, the distal plane normal is defined directly by α and β.

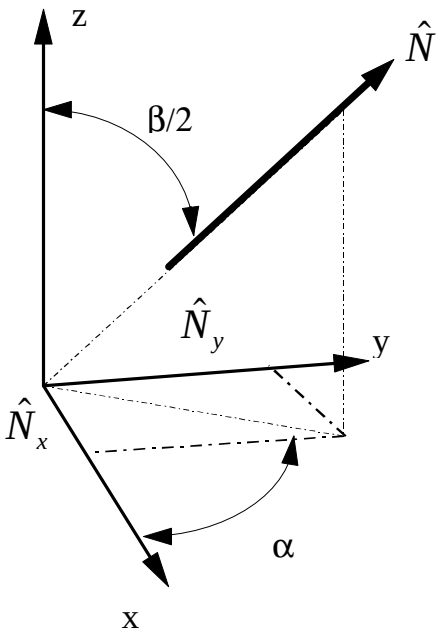

Figure 4.2: Midplane Normal

4.4 Singularity Analysis

It has been suggested that the Carpal Wrist contains a large, singularity-free workspace based on the position kinematics (Chap. 3) and observation of the prototype model. This claim will now be examined through a singularity analysis of the Jacobian. From the Jacobian previously developed, an equation for the determinant is derived as a function of the three input angles, θ_i, $i = 1, \ldots, 3$:

$$det[\mathbf{J}] = \begin{pmatrix} \left(\frac{\partial \hat{N}_x}{\partial \theta_1} * \frac{\partial \hat{N}_y}{\partial \theta_2} * \frac{\partial p_d}{\partial \theta_3} + \frac{\partial \hat{N}_x}{\partial \theta_2} * \frac{\partial \hat{N}_{y2}}{\partial \theta_3} * \frac{\partial p_d}{\partial \theta_1} + \frac{\partial \hat{N}_y}{\partial \theta_3} * \frac{\partial \hat{N}_y}{\partial \theta_1} * \frac{\partial p_d}{\partial \theta_2} \right) \\ -\left(\frac{\partial \hat{N}_x}{\partial \theta_3} * \frac{\partial \hat{N}_y}{\partial \theta_2} * \frac{\partial p_d}{\partial \theta_1} + \frac{\partial \hat{N}_x}{\partial \theta_1} * \frac{\partial \hat{N}_{y2}}{\partial \theta_3} * \frac{\partial p_d}{\partial \theta_2} + \frac{\partial \hat{N}_x}{\partial \theta_2} * \frac{\partial \hat{N}_y}{\partial \theta_1} * \frac{\partial p_d}{\partial \theta_3} \right) \end{pmatrix} \tag{4.23}$$

with the partial derivatives presented earlier.

Singular positions can be found by setting this determinant equal to zero and solving for θ_1, θ_2, and θ_3. This approach is common in locating singularities in serial devices. In serial robots, solving frequently leads to specific joint angle values that create singular positions of the manipulator. However, the three input angles in the Carpal Wrist determinant equation are coupled such that most of the singular positions are not obvious. A search for zeros of the determinant reveals two infinities of singular positions, i.e., the singular input values form a surface. For the wrist to be singularity free inside its workspace, this surface of singular positions must coincide or be outside the workspace boundary (the workspace boundary is defined by closure in the kinematic position equations).

A test was performed by evaluating det[**J**] for singular input values and then comparing these with kinematic closure (this is indicated by the inability of the mechanism to assemble which occurs when the discriminant goes to zero in the position solution) at these same values. A few sample results are shown in Table 4.2:

Table 4.2: Comparison of Singularity Measure and Kinematic Closure

θ_1 (deg)	θ_2 (deg)	θ_3 (deg)	Kinematic Closure: (***discriminant***)	Singularity Measure (det[**J**])
44.43	122.29	-24.66	1.986	0.0433
44.43	123.08	-24.81	0.6458	0.0249
44.43	123.53	-24.86	0.1996	0.0139
44.43	124.00	-24.88	0.0034	0.0018

These results illustrate that, as a singular position is approached (det[**J**]$\rightarrow$0), the workspace boundary is also approached (***discriminant***$\rightarrow$0). Figure 4.3 graphically illustrates these results. The kinematic parameters, base, leg and plunge lengths (Fig. 4.1), given by the dimensionless ratios, $R_b = b/l$ and $R_d = p_d/l$, determine the radius and size of the wrist's spherical workspace. For a 2-D slice of the workspace, the bending angle β (Fig. 4.2) is increased until the edge of the workspace is reached, as determined by loss of kinematic closure. This is plotted in Fig. 4.3. A similar procedure is implemented to find the bounds of the singular surfaces described above. For this case, β is increased until a singular position is reached. The results of this procedure are

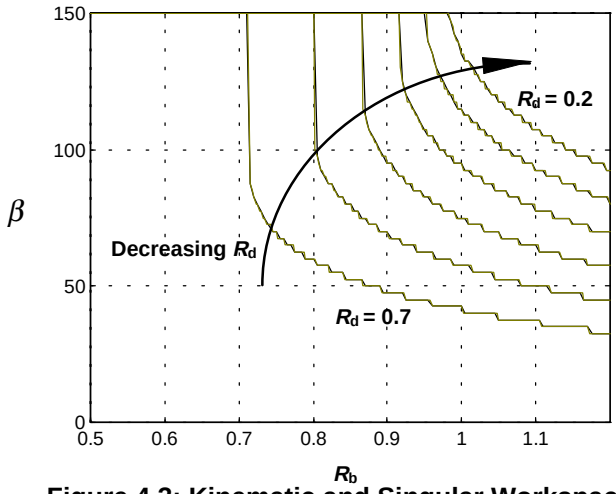

Figure 4.3: Kinematic and Singular Workspace Boundaries

also plotted in Fig. 4.3. As expected, the curves defining the two boundaries are nearly coincident, making it impossible to differentiate between the two in Fig. 4.3. This demonstrates that the edge of the singular workspace coincides with the edge of the kinematic workspace, verifying the singularity-free nature of the Carpal Wrist.

4.5 Dexterity Analysis

The dexterity of the Carpal Wrist will be characterized using two traditional quantitative definitions of dexterity: a determinant-based dexterity index, and a Jacobian matrix decomposition-based dexterity index. Using the determinant approach, det[**J**] gives a measure of the "size" of **J**, i.e. the size of the ratio going from the wrist inputs to the wrist outputs. However, each independent degree of freedom of a manipulator has its own contribution to the overall dexterity index. This is apparent since rows of the Jacobian matrix describe the effects of all inputs on each output velocity. It is thus possible to lose dexterity by losing the ability to move in one direction, while maintaining good movement ability in other directions. The second approach, the Jacobian-matrix singular value decomposition (SVD) provides additional insight of the physical system since it provides singular values and the corresponding direction vectors equal in number the dof of the manipulator. Using these two definitions of dexterity, the analysis was performed with a computer algorithm that provided graphical display of the results. The input parameters to the kinematic model for dexterity analysis are the dimensionless ratios, R_b and R_d, defined in Chap. 3 as:

$$R_b = b/l, \qquad R_d = p_d/l. \tag{4.24}$$

R_b fixes the size of the links in the wrist while R_d determines the radial size of the spherical workspace. Choosing values for these parameters, the Jacobian model is evaluated, and the two dexterity measures are calculated over the entire workspace. The numerical output is then used to produce a map of dexterity values. In evaluating the dexterity information, both kinematic closure and an upper bound on the singular-value ratio were checked to determine if a workspace

boundary had been reached. In a larger spherical workspace (larger R_d ratio), kinematic closure formed the workspace bound. On smaller spheres (smaller R_d values) the singular-value ratio cutoff indicated singular positions at the workspace edge. However, in all cases, both dexterity measures demonstrated a relatively uniform dexterity inside the workspace, and a loss of dexterity near the workspace edge.

Figure 4.4 demonstrates both dexterity measures for ratio values $R_b = 0.75$ and $R_d = 0.70$. Note that at the edge of the workspace, the determinant-based dexterity index (the lower surface in Fig. 4.4) approaches zero, while the singular-value dexterity index (the upper surface in Fig. 4.4) becomes very large. This illustrates the transition of the SVD ratio which rapidly increases to infinity at the workspace bounds. Figure 4.5 shows the determinant-based dexterity index for multiple R_d ratios. As the R_d value decreases, the dexterity region becomes larger (also demonstrated in Fig. 4.5). While only the determinant-based index is shown, the singular-value index was used as a cutoff for locating singular positions.

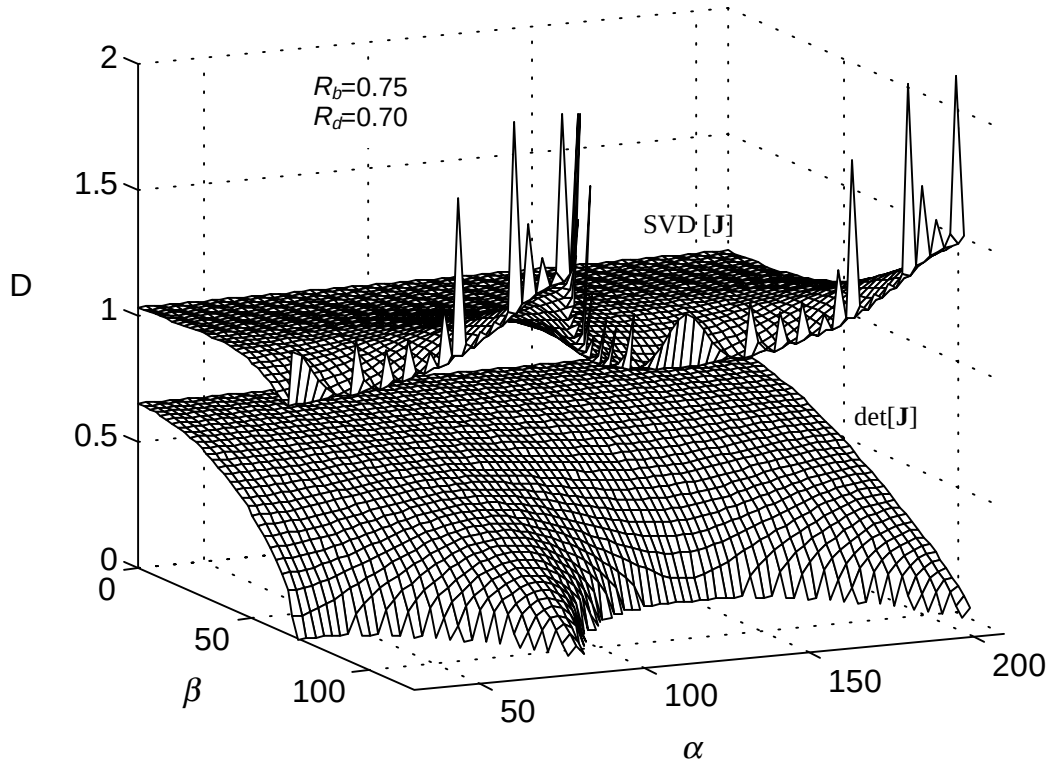

Figure 4.4: Dexterity Measures Plotted Over an Angular Representation of the Workspace.

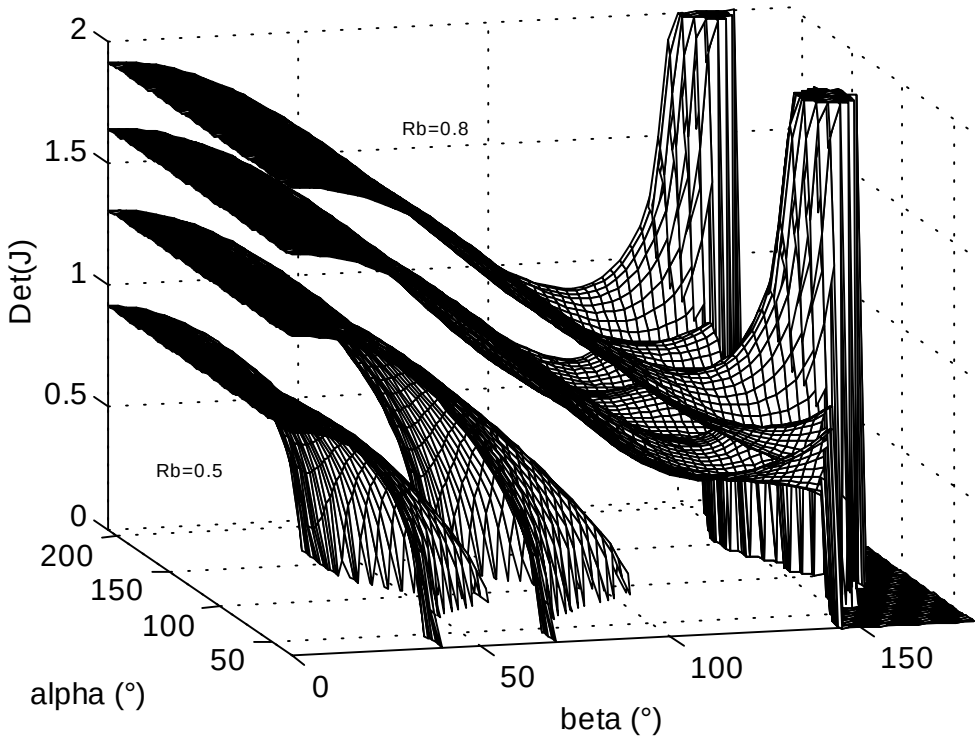

Figure 4.5: Determinant-Based Dexterity Plotted over the Workspace for Multiple R_d Ratios

4.6 Dexterous Manipulator Workspace

Robotic dexterity is a measure of a manipulator's ability to adequately and effectively position and orient a tool within its reachable workspace in a given direction. Since the ability to pose (position and orient) is the robot's fundamental task, the parameter for evaluating this, referred to as the "dexterous measure," is an extremely important parameter for use in selecting and evaluating manipulators. Here, uniformity in dexterity is demonstrated to be the correct basis for comparison of two or more manipulators, all other factors being equal. Uniformity of dexterity is the essential feature of a dexterous manipulator because of the ability to gear inputs through transmissions or driving elements and thus modify the scale or magnitude of dexterity. The relative magnitudes of the dexterity are always assumed to be corrected for at the actuator level, either by means of transmission gearing or in actuator selection. This dexterous measure is applied to the Carpal Wrist. Comparisons in this measure between the Carpal Wrist and other traditional pointing wrists are made for a general task over a nearly hemispherical workspace.

4.6.1 Approach to Dexterous Measure

While many specific definitions for position-dependent dexterity have been presented, only a few approaches for determining the dexterous measure of manipulators have been suggested. The approaches that do address an overall dexterous measure evaluate this as the size of the manipulator's workspace that meets certain criteria. In Craig (1989), the criteria is a lack of singularities, i.e., the volume of space which a robot can reach with all orientations. Paul and Stevenson (1983), Stanisic and Duta (1990), and Remis and Stanisic (1993) use the criteria of a minimum value (for example, 0.5) for the Jacobian determinant. They define a cone a degeneracy or singular cone as the region of workspace where this criteria fails, and the dexterous workspace as the remaining workspace. In the case of a non-square Jacobian, the determinant of $\mathbf{J}^{\mathbf{T}}\mathbf{J}$ is evaluated and compared to a minimum value (for example, $(0.5)^2$). A third criteria is a maximum number for the ratio of maximum to minimum singular values (Salerno, 1993). Yoshikawa (1985) proposes a measure of manipulability, based on the volume of the manipulability ellipsoid, an ellipsoid with principal axes the singular-value vectors from a singular-value decomposition of the Jacobian matrix. The volume of this ellipsoid is the product of the singular values and a constant defined by the number of degrees of freedom of the task. This approach is similar to defining the manipulability or dexterous measure as a workspace size, except that volume is now described in a new space derived through a singular-value decomposition of **J**.

4.6.2 Definition of Dexterous Measure

The dexterity, *D* is a function of the manipulator's position within the workspace as well as it's direction of velocity (or impending motion). The task of the robot defines both the position and velocity components. Therefore, any method of dexterity is path and task dependent (position-within-task dependent). Uniformity in the dexterity measure over the task, however is the key

parameter in defining the dexterous measure of the manipulator. In other words, a robot is dexterous if the chosen dexterity measure is relatively uniform over the task-specified workspace of the manipulator. The abbreviated definition of the dexterous measure of a presents essence of the idea of a manipulator being dexterous. That, when considered in terms of some specific or general task, it is most desirable to have a manipulator (or any other mechanical device) with a uniform output to input velocity ratio, i.e., a uniform mechanical advantage. More important than a specific dexterity value at a position in the workspace, this uniform dexterous measure of manipulators will aid in evaluating potential robotic devices for application. When a manipulator satisfies the requirements of being sufficiently dexterous, a specific level or magnitude of dexterity can be incorporated through transmission elements in the actuation components. Uniformity in dexterity will be measured as the standard deviation of the chosen position-dependent dexterity measurement.

4.6.3 Application to Three Pointing Manipulators

The dexterous measure of Carpal Wrist will be evaluated and compared to two similar pointing manipulators: a serial pitch-yaw manipulator, and the spherical five-bar parallel drive linkage. For uniformity in comparison, all three manipulators will perform the same task over the same, hemispherical workspace. The output velocity space will be the pointing direction, a two degree-of-freedom orientational specification, for each manipulator (all Jacobians will have two rows). The task is a simple pointing operation. For this pointing task, dexterity will be defined to evaluate the worst case pointing direction for every position in the workspace (minimum singular value defines the dexterity). Standard deviation of this minimum principle dexterity over the workspace gives the dexterous measure for each manipulator to be compared. Note that the serial pitch-yaw and the spherical five-bar have two inputs, yielding square Jacobians, while the Carpal Wrist has three inputs yielding a non-square, “short and fat” Jacobian.

First, the kinematic position and velocity equations of each manipulator are presented (the Carpal Wrist kinematics have been presented in chaps. 3 and 4). Then, the specified position-dependent dexterity definition is applied to all three manipulators. Also, a single, constant gearing ratio (Eq. 5) is applied to each manipulator as needed to result in an equivalent, normalized scale of dexterity.. Using the resulting system Jacobians, the dexterity is evaluated and mapped over the hemispherical workspace. The dexterous measure is calculated from this map as the standard deviation of the position-dependent dexterity.

4.6.3.1 Carpal Wrist

Start with the Carpal Wrist Jacobian, which was given in section 4.0 and 4.3 as Eqs. (4.2) and (4.12):

$$\mathbf{v}_{cw} = \mathbf{J}\omega\,; \qquad \mathbf{J} = \begin{bmatrix} \partial\hat{N}_x/\partial\theta_1 & \partial\hat{N}_x/\partial\theta_2 & \partial\hat{N}_x/\partial\theta_3 \\ \partial\hat{N}_y/\partial\theta_1 & \partial\hat{N}_y/\partial\theta_2 & \partial\hat{N}_y/\partial\theta_3 \\ \partial p_d/\partial\theta_1 & \partial p_d/\partial\theta_2 & \partial p_d/\partial\theta_3 \end{bmatrix}. \tag{4.25}$$

For this analysis, the output velocity vector is the time rate of change of the spherical coordinates, α and β:

$$\mathbf{v} = \begin{Bmatrix} \dot{\alpha} \\ \dot{\beta} \end{Bmatrix}. \tag{4.26}$$

The Carpal wrist Jacobian given above is operated on by the transform matrix, **T** to give the desired output velocities:

$$\begin{Bmatrix} \dot{\alpha} \\ \dot{\beta} \end{Bmatrix} = \mathbf{T} \begin{Bmatrix} \dot{N}_x \\ \dot{N}_y \end{Bmatrix}, \quad \mathbf{T} = \begin{bmatrix} \dfrac{-N_y}{N_x^2 + N_y^2} & \dfrac{N_x}{N_x^2 + N_y^2} \\ \dfrac{N_x}{N_z\sqrt{N_x^2 + N_y^2}} & \dfrac{N_y}{N_z\sqrt{N_x^2 + N_y^2}} \end{bmatrix} \tag{4.27}$$

The transform operation,

$$\begin{Bmatrix} \dot{\alpha} \\ \dot{\beta} \\ \dot{p} \end{Bmatrix} = \begin{bmatrix} & \mathbf{T} & & 0 \\ & & & 0 \\ 0 & 0 & 1 \end{bmatrix} \mathbf{J} \begin{Bmatrix} \dot{\theta}_1 \\ \dot{\theta}_2 \\ \dot{\theta}_3 \end{Bmatrix} \tag{4.28}$$

where $\dot{p}$ is the time rate of change of the plunge distance. Finally, the upper 2x3 submatrix, $\tilde{\mathbf{J}}$ is extracted from **J** to relate **v** to the input actuator velocities.

$$\begin{Bmatrix} \dot{\alpha} \\ \dot{\beta} \end{Bmatrix} = \tilde{\mathbf{J}} \begin{Bmatrix} \dot{\theta}_1 \\ \dot{\theta}_2 \\ \dot{\theta}_3 \end{Bmatrix}; \tilde{\mathbf{J}} = \begin{bmatrix} J_{1,1} & J_{1,2} & J_{1,3} \\ J_{2,1} & J_{2,2} & J_{2,3} \end{bmatrix} \tag{4.29}$$

For this pointing task, the minimum singular value is evaluated from $\tilde{\mathbf{J}}$ and plotted over the hemispherical workspace as shown in Fig. 4.8. The standard deviation of this dexterity map is calculated resulting in a dexterous measure of σ_{dext} = 0.0375 (Table 4.3).

Table 4.3: Results of Dexterous Measure Evaluation

Wrist Type	D_{min}	D_{min}	$\sigma_{n-1}(D_{min})$
Carpal Wrist	0.45	~0.61	0.0375
Serial Pitch-Yaw	0.1	~1.0	0.2047
Pointing Five-Bar	0.7	~1.2	0.1249

4.6.3.2 Serial Pitch-Yaw Wrist

The serial pitch yaw wrist is an architecture commonly used in many industrial robots such as PUMA ®, Adept ™, and Staubli ™. This wrist has a simple kinematic configuration, shown in Fig. 4.6, with two actuated input parameters, θ_1 and θ_2.

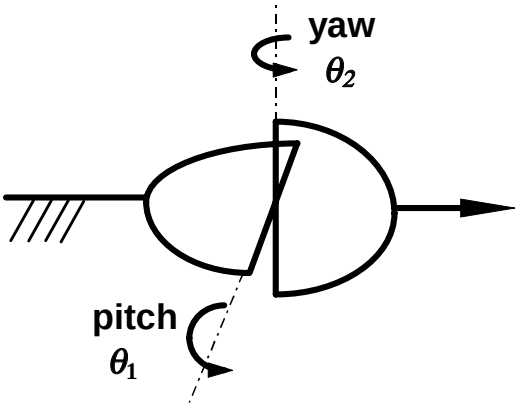

Figure 4.6: Serial Pitch-Yaw Wrist

The forward kinematic solution solves for the pointing direction vector, **N**, as a function of the input angles:

$$\begin{Bmatrix} N_x \\ N_y \\ N_z \end{Bmatrix} = \begin{Bmatrix} \sin\theta_2 \cos\theta_1 \\ -\sin\theta_1 \\ \cos\theta_2 \cos\theta_1 \end{Bmatrix} \tag{4.30}$$

The inverse kinematic solution solve the required input angles given a specific output pointing direction, in this case in terms of the spherical coordinates, α and β:

$$\begin{aligned} N_x &= \sin\beta\cos\alpha \\ N_y &= \sin\beta\sin\alpha \end{aligned} \tag{4.31}$$

$$\begin{aligned} \theta_1 &= \sin^{-1}(-\sin\beta\sin\alpha) \\ \theta_2 &= \sin^{-1}\left(\frac{\sin\beta\cos\alpha}{\cos\theta_1}\right) \end{aligned} \tag{4.32}$$

The velocity analysis is carried out by differentiation and yields the serial pitch-yaw wrist Jacobian relating the output velocities, $\dot{\alpha}$ and $\dot{\beta}$ to the input actuator velocities.

$$\begin{Bmatrix} \dot{\alpha} \\ \dot{\beta} \end{Bmatrix} = \mathbf{J}\begin{Bmatrix} \dot{\theta}_1 \\ \dot{\theta}_2 \end{Bmatrix} = \begin{bmatrix} \dfrac{-N_y}{N_x^2+N_y^2} & \dfrac{N_x}{N_x^2+N_y^2} \\ \dfrac{N_x}{N_z\sqrt{N_x^2+N_y^2}} & \dfrac{N_y}{N_z\sqrt{N_x^2+N_y^2}} \end{bmatrix} \begin{bmatrix} -\sin\theta_1\sin\theta_2 & \cos\theta_1\cos\theta_2 \\ -\cos\theta_2 & 0 \end{bmatrix} \begin{Bmatrix} \dot{\theta}_1 \\ \dot{\theta}_2 \end{Bmatrix} \tag{4.33}$$

For the pointing task, the minimum principal dexterity is calculated and plotted over the hemispherical workspace as shown in Fig. 4.9. The standard deviation of these values gives the dexterous measure of the serial pitch-yaw wrist as $\sigma_{dext} = 0.2047$.

4.6.3.3 Spherical Five-Bar Pointer

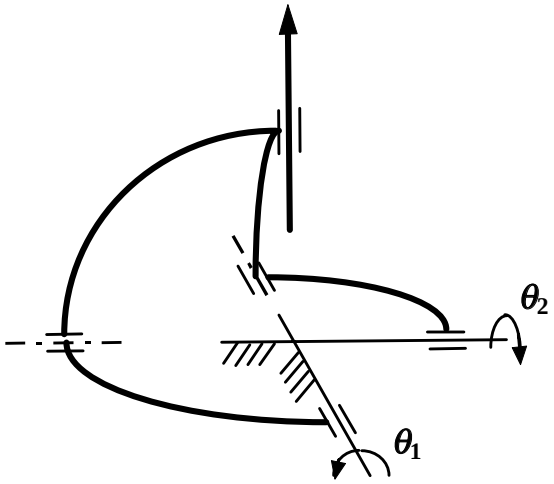

Figure 4.7: Spherical Five-Bar Parallel-Actuated Linkage

The spherical five-bar parallel drive linkage was analyzed by Ouerfelli and Kumar (1991). A special geometry of this device, shown in Fig. 4.7, which has the two actuated links perpendicular to each other and all four links spanning one quadrant or 90 degrees, will be evaluated. For this special geometry, the forward kinematic geometry is:

$$\begin{matrix} N_x = \sin\theta_1 \\ N_y = \sin\theta_2 \end{matrix}, \quad \begin{matrix} \alpha = \tan^{-1}\left(\sin\theta_2 \big/ \sin\theta_1\right) \\ \beta = \sin^{-1}\left(\sqrt{\sin^2\theta_1 + \sin^2\theta_2}\right) \end{matrix} \tag{4.34}$$

and the inverse kinematics:

$$\begin{aligned} \theta_1 &= \sin^{-1}(\sin\beta\sin\alpha) \\ \theta_2 &= \sin^{-1}(\sin\beta\sin\alpha) \end{aligned} \tag{4.35}$$

Differentiating the output space coordinates results in the spherical five-bar Jacobian:

$$\begin{Bmatrix} \dot{\alpha} \\ \dot{\beta} \end{Bmatrix} = \mathbf{J}\begin{Bmatrix} \dot{\theta}_1 \\ \dot{\theta}_2 \end{Bmatrix} = \begin{bmatrix} \dfrac{-\sin\beta\sin\alpha}{(\sin\beta\cos\alpha)^2 + (\sin\beta\sin\alpha)^2} & \dfrac{\sin\beta\cos\alpha}{(\sin\beta\cos\alpha)^2 + (\sin\beta\sin\alpha)^2} \\ \dfrac{\sin\beta\cos\alpha}{den} & \dfrac{\sin\beta\sin\alpha}{den} \end{bmatrix} \begin{bmatrix} \cos\theta_1 & 0 \\ 0 & \cos\theta_2 \end{bmatrix} \begin{Bmatrix} \dot{\theta}_1 \\ \dot{\theta}_2 \end{Bmatrix} \tag{4.36}$$

with:

$$den = \sqrt{(\sin\beta\cos\alpha)^2 + (\sin\beta\sin\alpha)^2}\sqrt{1 - (\sin\beta\cos\alpha)^2 - (\sin\beta\sin\alpha)^2}$$

Again, the spherical five-bar Jacobian is evaluated over a hemispherical workspace, mapping the minimum singular values, and then taking the standard deviation over the entire workspace for its dexterous measure to give a dexterous measure of σ_{dext} = 0.1249. Figure 4.10 shows the minimum principle dexterity map over the hemispherical workspace.

4.6.4 Dexterous Measure Results

With the kinematics and dexterity equations generated the three manipulators were evaluated on over a hemispherical pointing direction workspace. Figs. 4.8, 4.9, and 4.10 show the minimum principal dexterity plotted over the hemispherical workspace of the Carpal Wrist, the serial pitch-yaw wrist, and the spherical five-bar pointer respectively. Table 4.3 summarizes the evaluation of the minimum principal dexterity and maximum and minimum values. Also shown is the standard deviation of the minimum dexterity which is the dexterous measure for each of the manipulators.

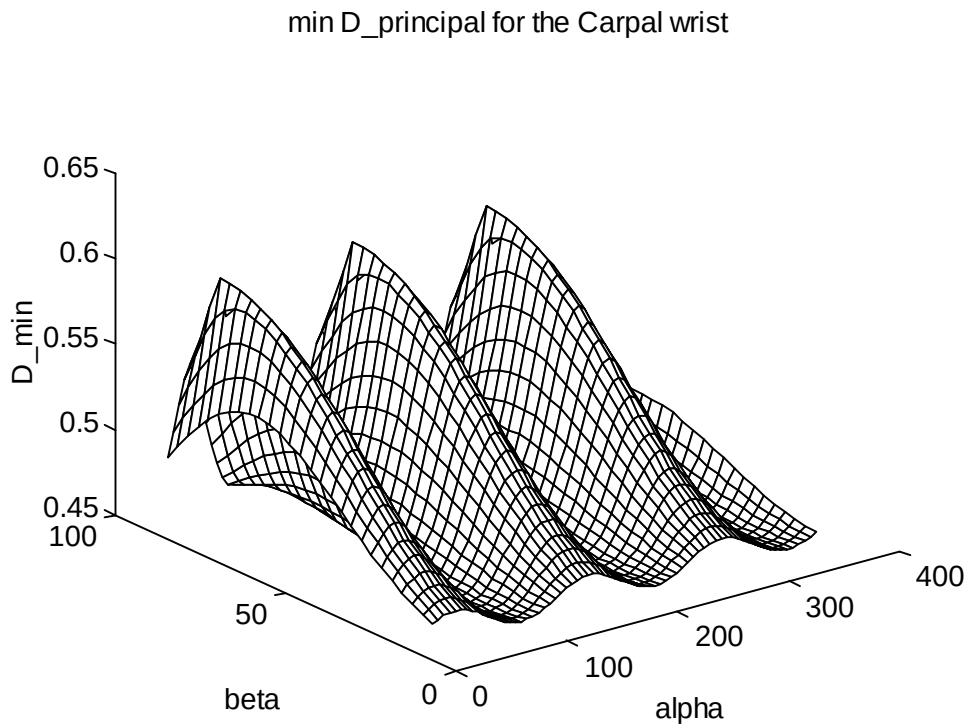

Figure 4.8: Minimum Dexterity Plot of the Carpal Robotic Wrist

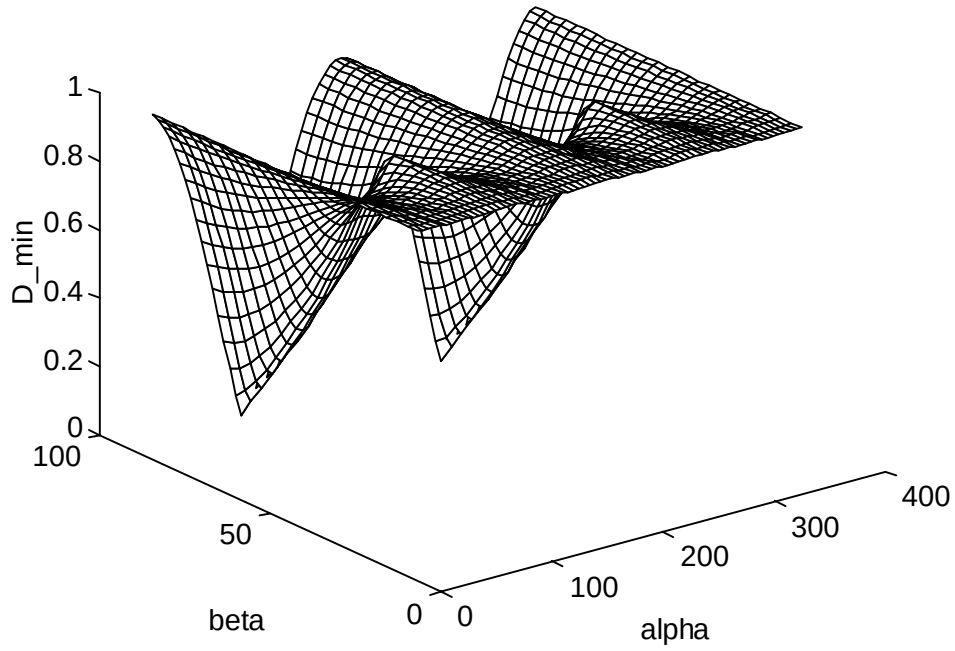

Figure 4.9: Minimum Dexterity Plot of Serial Pitch-Yaw Wrist

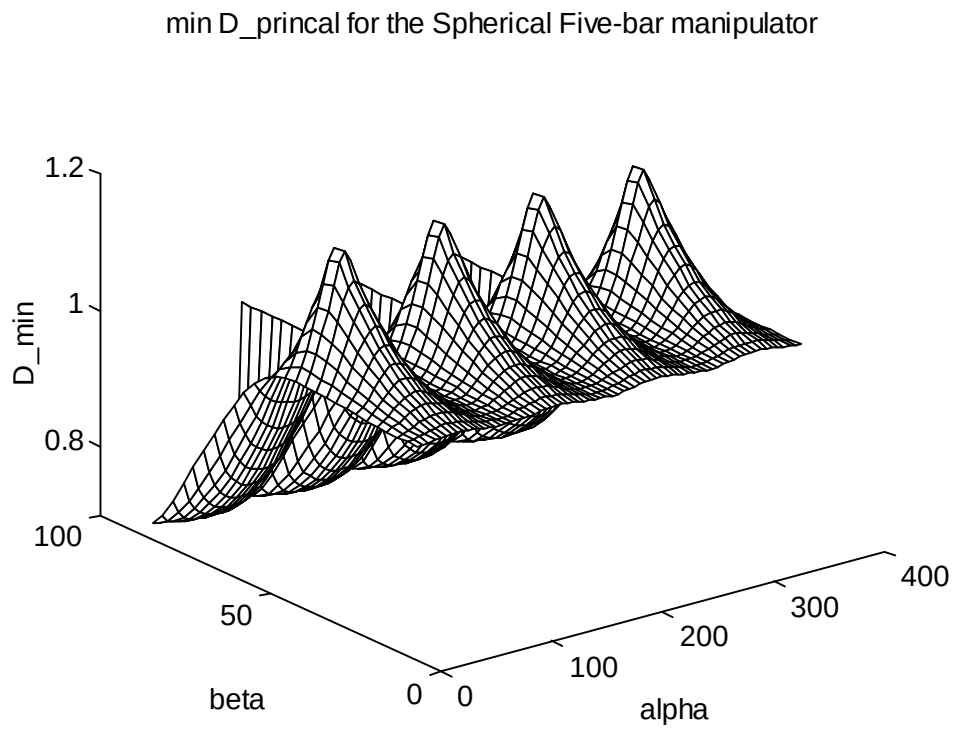

Figure 4.10: Minimum Dexterity Plot of Spherical Five-Bar Linkage

4.7 Conclusions

The instantaneous kinematics of the Carpal wrist are presented in a closed-form Jacobian, which expresses the output velocities as a linear function of the three input angular velocities. This Jacobian is used to carry out a singularity and dexterity analysis of the Carpal Wrist. The results of these analyses, using determinant-based and singular-value decomposition-based dexterity definitions are reported graphically on Figs. 4.3 - 4.5, demonstrate the large, singularity-free workspace of the Carpal Wrist. The multiple plots on Fig. 4.5 show the Carpal Wrist to have a continuous, solid angle workspace of greater than 180 degrees at R_d ratios less than 0.6, while maintaining a good state of dexterity. The dexterous measure, the measure of uniformity in dexterity, was then presented as the best overall evaluation of the instantaneous kinematic performance of a manipulator. This dexterous measure provides a means in comparing and selecting manipulators based on a standard task and dexterity definition. The definition of the dexterous measure provides versatility in three ways: freedom to evaluate over a specific task or a general task, freedom in choice of dexterity parameter that best matches the task, and choice of evaluating uniformity. When a manipulator is determined to be dexterous using this measure, the magnitude of dexterity becomes less significant since it may be modified to meet the task. Based on the dexterity definition given in Eq. 4.3, (Soper et al., 1997), the Carpal Wrist was compared to two other similar pointing manipulators. The results of this comparison, shown in Figs. 4.8, 4.9, and 4.10, and Table 4.3, demonstrate the Carpal Wrist to be superior in uniformity in workspace dexterity.